Soft Glassy Dynamics in Polypropylene−Clay Nanocomposites

Mark A. Treece and James P. Oberhauser*

Department of Chemical Engineering, University of Virginia, Charlottesville, Virginia 22904

Received June 2, 2006; Revised Manuscript Received November 10, 2006

ABSTRACT: Linear and nonlinear viscoelastic measurements were utilized to probe transient morphological changes in a melt-blended polypropylene−clay nanocomposite containing 3 wt % organically modified montmorillonite clay, 10 wt % maleic anhydride functionalized polypropylene (1% maleic anhydride content), and 87 wt % polypropylene homopolymer. Steady shear rate sweeps show that the viscosity decreases monotonically with shear rate, characteristic of a mechanically percolated material with a yield stress. Subsequent sweeps following annealing of up to 2 h show that the viscosity at low shear rates remains substantially lower than the initial sweep, indicative of slow or arrested organoclay disorientation. In startup of shear flow, as-processed and presheared nanocomposite samples both exhibit increasing viscosity overshoots with annealing time for up to 6 h, although the overshoots for the presheared samples remain uniformly smaller than those of the as-processed material. Similarly, small-amplitude oscillatory shear experiments on as-processed and presheared samples also reveal that the storage modulus and complex viscosity increase logarithmically with time, while the loss tangent declines steadily. Both sets of data point to increasingly solidlike rheology over time, a phenomenon that is discussed in the context of soft glassy dynamics.

I. Introduction

Polymer−clay nanocomposites (PCNs) have recently attracted significant attention due to marked property enhancements at mass loadings substantially less than conventional fillers. For instance, increased tensile strength and modulus along with improved permeation resistance, flame retardation, and heat distortion characteristics have all been reported for many common polymers with the addition of only a few weight percent clay.[1−6] These remarkable property enhancements make PCNs superior candidates for materials applications in the food packaging, electronics, and automotive industries. The smectic clay montmorillonite (MMT) is commonly used as the inorganic component in PCNs. MMT has a highly anisotropic, layered silicate structure, where the layer thickness is 0.98 nm and the lateral dimension is a few hundred nanometers. Individual layers are separated by a charged intergallery, which causes it to be hydrophilic in its native state. Consequently, surface modification of the clay is necessary in order to render it organophilic and, therefore, miscible with hydrophobic polymers. Surface modification is typically achieved via cation exchange reactions using primary, secondary, tertiary, and quaternary alkylammonium surfactants.[7] Through this modification, the clay intergallery is expanded, allowing improved chemical and physical interaction between the organically modified clay (or organoclay) and polymer. However, for highly nonpolar polymers (e.g., polypropylene), the unfavorable enthalpic interaction between polymer and organoclay prohibits diffusion of polymer into swollen intergalleries despite the reduced entropic penalty for doing so. As a result, it is customary to add a compatibilizer, which for polypropylene is often a low molecular weight copolymer of polypropylene and maleic anhydride (PP-*g*-MA). PP-*g*-MA interacts with clay through hydrogen bonding between its polar functional group and the oxygen group of the clay silicates.[8] Hence, by organically modifying the clay surface and adding a compatibilizer, one can significantly improve the chemical interaction between a hydrophobic polymer and clay and promote the exfoliated organoclay morphology associated with maximum interfacial area between the silicate and polymer matrix, which is critical to macroscopic material property enhancement.

For nonpolar polymers like polyolefins, melt-blending offers the most convenient and cost-effective means of preparing PCNs, and recent work has connected extruder type, screw design, and shearing conditions with degree of exfoliation and dispersion of organoclay in polymer melts.[9−11] Hence, a fundamental understanding of the relationship between deformation and microstructure in the molten state is critical. A number of experimental techniques have been used to characterize the microstructure of PCNs, the most common being X-ray diffraction (XRD) and transmission electron microscopy (TEM). However, while XRD and TEM provide important information on the mean spacing between clay silicate layers and a qualitative view of microstructure by direct visualization, respectively, they are solid-state measurements that offer only an instantaneous view of structure. On the other hand, the relationship between the rheological properties of particulate-filled materials and the volume fraction of particles, particle shape and size, and particle−polymer interactions is well-documented.[12] Although rheology provides only an indirect probe of microstructure, its sensitivity to the time-dependent mesoscale structure observed in several PCN systems makes it an invaluable complementary analytical tool.[13−24]

Of particular interest are the studies focusing on the linear and nonlinear rheological response of PCNs. Because the polymer matrices used are diverse [e.g., nylon-6,[13,25] polypropylene (PP),[21−23,26−28] polystyrene (PS),[24,29−31] poly(ϵ-caprolactone),[13,32,33] polystyrene−polyisoprene (PS−PI) block copolymers,[18,34] and polystyrene−polyisobutylene (PS−PIB) block copolymers],[20] the rheological signatures are believed to be largely universal. For example, in the linear viscoelastic regime, several researchers have performed small-amplitude oscillatory shear (SAOS) experiments and reported a change in terminal behavior from a liquidlike response for unfilled polymers [i.e., storage (G') and loss (G'') moduli related to angular frequency (ω) according to the relations $G' \propto \omega^2$ and $G'' \propto \omega$] to a solidlike

* To whom correspondence should be addressed: e-mail oberhauser@virginia.edu; telephone (434) 924-7974; fax (434) 982-2658.

10.1021/ma0612374 CCC: $37.00
Published on Web 01/13/2007

response for PCNs (i.e., G', $G'' \propto \omega^0$). Similar behavior has been noted for carbon black,[35,36] calcium carbonate,[37] and talc[38] filled polymers, although in those cases the particle volume fractions were substantially higher than the 1−2 vol % for which solidlike behavior is seen for PCNs. The onset of the solidlike terminal response has been attributed to dispersed organoclay domains forming a three-dimensional percolated network mesostructure.[15,20−22,26,27] Such domains may include individual exfoliated silicate layers as well as intercalated stacks referred to as tactoids.

Moreover, intriguing but conflicting time-dependent terminal behavior has also been observed. Ren et al.[20] examined the recovery of the storage modulus at fixed low frequency following prolonged large-amplitude oscillatory shear (LAOS) alignment of organoclay domains and witnessed a logarithmic increase in time, independent of the molecular weight and viscosity of the polymer matrix, type of organoclay, and effective dispersion. The authors also noted that the postshear modulus remained substantially smaller than that before shear alignment even after several hours, suggesting that the disorientation kinetics of aligned organoclay domains are slower than Brownian motion would permit and perhaps even arrested prematurely. Alternatively, Galgali et al.[22] conducted sequential SAOS frequency sweeps on otherwise unsheared PP−clay samples with and without PP-*g*-MA compatibilizer. They reported a *decrease* in the storage and loss modulus with increasing annealing time. At the same time, the zero-shear viscosity measured under creep *increased* logarithmically with annealing time, in apparent contradiction to the decrease with time one would have inferred from the moduli. Despite the inconsistencies, these data indicate that subtle microstructural changes occur over very long time scales in both as-processed and presheared samples.

The steady shear behavior of PCNs has also been examined, although to a somewhat lesser degree.[14,19,21,25] The empirical Cox−Merz rule, which is widely accepted for homopolymers, fails for PCNs, particularly at organoclay loadings above the mechanical percolation threshold. The steady shear viscosity fails to exhibit a plateau at low shear rates and instead continuously shear thins over the entire shear rate range tested. Such behavior suggests an apparent yield stress and also indicates that flow-induced alignment of organoclay domains is readily accomplished under steady shear.[15,19] Additionally, Solomon et al.[21] performed nonlinear reversing shear flow experiments in order to study the transient structural evolution during shear and the disorientation kinetics of flow-aligned organoclay domains during the annealing period between deformations. Noting the increasing magnitude of the shear stress overshoot with annealing time and the dependence of that overshoot on strain (not strain rate), they concluded that the organoclay microstructure was not only evolving during annealing but doing so in a non-Brownian fashion. The authors argue that organoclay domains form a weakly agglomerated structure that may be ruptured by flow and reconstituted through attractive interactions upon cessation of shear.

Central to the discussion of organoclay disorientation kinetics and relaxation in PCNs is the analogy to the dynamics of soft colloidal glasses put forth by Ren et al.[20] Glassy colloidal suspensions have mechanical properties similar to metastable soft solids (e.g., solidlike behavior with a finite yield stress, thixotropy under deformation, and slow recovery from a deformation), properties that may evolve continuously over time.[39−45] The continuous time evolution of mechanical properties is an "aging" phenomenon characteristic of systems that are far from equilibrium[46] and associated with the metastable, heterogeneous structure of soft materials on microscopic to mesoscopic length scales.[47,48] It has been hypothesized that structural disorder creates energy barriers (like those associated with the rearrangement of droplets in an emulsion) that prevent reorganization into states of lower free energy, and those energy barriers become greater the longer a system is aged such that the longest relaxation time continuously increases. As a result, thermal motion alone is insufficient to mediate complete structural relaxation, and the system may become trapped in a higher energy state. The imposition of a deformation, however, is postulated to interrupt aging and rejuvenate the energy landscape, analogously to increasing the temperature above the glass transition.[44,49,50] Upon cessation of shear, aging begins anew; however, because flow may alter the energy landscape, new metastable states are now accessible, and the rheological signature of aging may change as well.

Fielding et al.[48] point out that aging effects in soft materials are seldom reported and instead viewed as artifacts obfuscating the "true" behavior of the material. Melt-blended PCNs should be inherently out-of-equilibrium, having experienced intense shearing and subsequent rapid cooling. Consequently, the time-dependent phenomena described previously as characteristic of soft glassy aging dynamics are germane to fundamental PCN research and industrial processing in that they impact macroscopic material properties. This study focuses upon a single melt-blended, compatibilized PP−clay nanocomposite sample that exhibits strongly time-dependent rheology. Inspired by the work of Solomon et al. and Ren et al., we report a unified approach to examining transient rheological behavior. We seek to not only resolve the conflicting results of Galgali et al. but also consider the rheological features common to all PCNs as opposed to those that are specific to a given polymer/surfactant chemistry. Since the polymer and surfactant chemistry may dictate the morphology of the hypothesized mesoscale organoclay network similarly to pH and ionic strength in Laponite dispersions, the analogy to colloidal gels and glasses will be discussed. Both SAOS, steady shear, and a combination of the two are employed in order to contrast the aging behavior of as-processed (i.e., unsheared) and presheared (i.e., flow-aligned) samples and elucidate the influence of time, thermal, and deformation history.

II. Experimental Section

Materials and Characterization. Polypropylene (PP, Dow Chemical grade H700-12, MFI = 12 g/10 min at 230 °C and 2.16 kg load, M_w = 229 000 g/mol, M_w/M_n = 3.98) was used as the matrix polymer. Southern Clay Products provided Cloisite 15A (C15A, 125 mequiv/100 g, d_{001} = 31.5 Å), a natural MMT clay modified with a ditallow quaternary ammonium salt. Polybond 3200 (PP-*g*-MA, Crompton Corp., MFI = 110 g/10 min at 190 °C and 2.16 kg load), a 1 wt % maleic anhydride functionalized polypropylene, was used as the compatibilizer. The nanocomposite was melt-blended in a Brabender twin-screw extrusion system (D6/2 with universal mixing screw). The dry-mixed sample consisted of 3 wt % C15A, 10 wt % PP-*g*-MA, and 87 wt % PP. Extrusion was performed with barrel temperatures ranging from 190 to 210 °C, and material was cycled through the extruder twice to promote mixing and dispersion of the clay.

X-ray diffraction (Scintag XDS 2000 diffractometer with Cu K_α radiation source at λ = 1.541 Å) was performed on 1.5 mm thick compression-molded PCN samples. The increased basal spacing (d_{001} = 34.5 Å) relative to the pure organoclay suggests that the extrusion process promoted some degree of intercalation and exfoliation, though exfoliation cannot be independently confirmed with XRD. Transmission electron microscopy (JEOL 2000FX

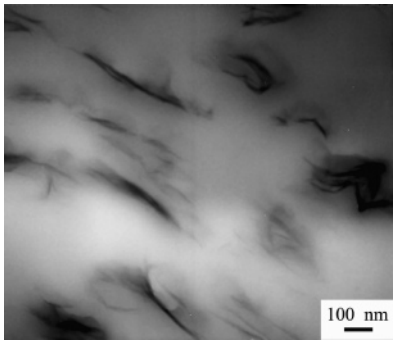

Figure 1. Bright-field TEM image of the 3 wt % polypropylene−clay nanocomposite at 60 000 times magnification, showing mostly intercalated organoclay domains of various sizes.

operated at 200 kV) was performed on ultra-microtomed sections (70−90 nm thick) to visually observe the clay dispersion. As seen in Figure 1, TEM affirms that the nanocomposite contains predominantly intercalated organoclay domains of various sizes. However, it is important to note that the number of organoclay domains appearing in the image is consistent with estimates based upon the volume fraction of organoclay and the TEM sample thickness, which speaks to the efficacy of the dispersion created by the melt-blending process.

Rheology. Three types of rheological experiment were employed to investigate the influence of time, thermal, and deformation history on the mesoscale organoclay network. All experiments were conducted with a TA Instruments AR 2000 rheometer equipped with a 25 mm parallel plate geometry and environmental test chamber. A nitrogen purge of 10 L/min was continuously supplied to inhibit thermo-oxidative degradation of PP during experiments. Compression-molded samples (190 °C for 10 min) were initially melted at 210 °C for 10 min in the rheometer, after which the upper plate was lowered to a gap distance of 1 mm for testing.

First, nonlinear rheology was probed using consecutive steady shear rate sweeps (0.01−1 s^{-1}), which were conducted at 180 °C with various annealing times (5−120 min) between each sweep. All sweeps were performed from low to high shear rates. Previous work has shown that PCNs above the mechanical percolation threshold behave as continuously shear-thinning, finite yield stress materials.[14,19,21,51] In particular, the materials shear thin at low shear rates where the matrix polymer would exhibit a zero-shear viscosity plateau. A series of shear rate sweeps enable one to monitor changes in the steady shear viscosity as a function of annealing time.

Next, inspired by the work of Solomon et al.,[21] startup of steady shear flow experiments were performed on both as-processed and presheared samples. In the former, the nanocomposite sample was melted as described above, annealed quiescently for different times (5−330 min) and temperatures (180 and 210 °C), and subsequently sheared at a rate of 0.1 s^{-1} in order to monitor the transient viscosity (or shear stress) overshoot. While the experiment could have been replicated at other shear rates in the linear viscoelastic regime of the polymer, the dependence of the overshoot on strain (not time), as observed by Solomon et al.,[21] suggests that a single shear rate is representative of the hydrodynamic response. Figure 2 shows a characteristic response of the viscosity (normalized by the steady shear viscosity at 0.1 s^{-1}) to startup of steady shear flow for the nanocomposite and the matrix polymer. Importantly, the polymer fails to exhibit an overshoot at this shear rate, indicating that the response is caused solely by the inclusion of the organoclay. Experiments at other shear rates confirm that the overshoot occurs at a fixed strain and emphasize the hydrodynamic origin of the response. In the same vein, flow reversal experiments are commonly used to probe the structure of textured materials like liquid crystal polymers[52−56] and rigid-rod suspensions[57] as well as immiscible polymer blends[58−60] and entangled homopolymers.[61−63] In these presheared experiments, the sample was melted and then immediately sheared at a rate of 0.1 s^{-1} at 180 °C until the viscosity reached steady state (5 min). The sample was then annealed for

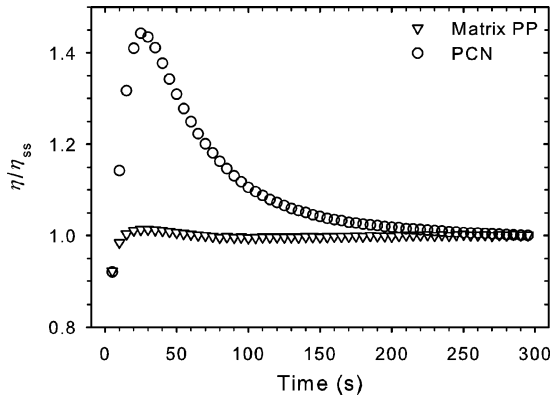

Figure 2. Plot of transient viscosity scaled by steady state viscosity in startup of shear flow for the 3 wt % nanocomposite and PP matrix polymer. Samples were annealed for 5 min at 210 °C prior to imposition of 0.1 s^{-1} shear rate at 180 °C. The overshoot in viscosity for the nanocomposite is a purely hydrodynamic response caused by the presence of anisotropic organoclay domains.

various times and temperatures before the same 0.1 s^{-1} shear rate was imposed in the reverse direction. The transient overshoot of the viscosity was again monitored. It should be noted that the startup flow experiments were performed at both 180 and 210 °C and the data averaged, since the resulting overshoots were found to be independent of the temperature during shear. Similarly, although the initial deformation of the presheared experiments was always performed at 180 °C, the reversing shear results were also averaged for both temperatures.

Finally, a series of SAOS experiments were performed to examine the transient nature of the organoclay network as evidenced by changes in the terminal behavior. As discussed earlier, several rheological studies of PCNs have revealed solidlike behavior in the storage modulus in the terminal regime. To explore the time dependence of the terminal response, consecutive frequency sweeps at 1% strain were performed for up to 10 h at 180 and 210 °C on both the matrix polymer and the nanocomposite. Oscillatory stress sweeps at 1 Hz confirm that 1% strain is well within the linear viscoelastic regime of both the nanocomposite and matrix polymer. Additionally, the SAOS sweeps were performed on both as-processed and presheared samples to investigate the effect of deformation history on the terminal response. The presheared samples were deformed according to the procedure described for the startup flow experiments (0.1 s^{-1} at 180 °C for 5 min). A higher preshear rate of 0.5 s^{-1} was also imposed prior to SAOS sweeps in order to further elucidate the effect of deformation strength on the time-dependent behavior. These results were supplemented by continuous oscillatory shear at fixed frequency for as-processed and presheared samples held at 180 and 210 °C. At 180 °C, the frequency was chosen to be 0.01 Hz; applying time−temperature superposition, the frequency at 210 °C was selected to be 0.0147 Hz.

III. Results

Steady Shear Rate. As previously discussed, particle loading drastically alters the steady shear rheological response, particularly once the mechanical percolation threshold has been exceeded.[19] The results of consecutive shear rate sweeps of the 3 wt % nanocomposite are shown in Figure 3. Here, the divergent viscosity at low shear rates for the initial sweep indicates that the sample is above the percolation threshold and characterized by a finite yield stress. In order to determine the yield stress of the sample, the low shear rate data for the shear stress (σ_{12}) are fitted to Casson's equation,[19,64] given by

$$\sigma_{12}^{1/2} = \sigma_0^{1/2} + a\dot{\gamma}^{1/2} \quad (1)$$

where σ_0 is the yield stress, $\dot{\gamma}$ is the shear rate, and a is an arbitrary constant. Doing so, the yield stress for this 3 wt %

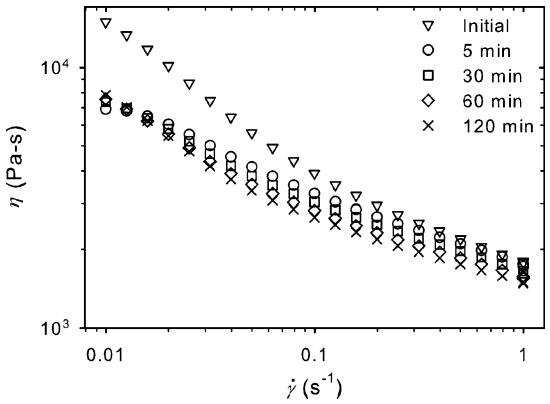

Figure 3. Steady shear rate sweeps of the 3 wt % nanocomposite followed by repeated sweeps performed after various annealing times. All experiments were conducted at 180 °C.

nanocomposite is estimated to be 87.1 Pa. For completeness, we point out that the matrix polymer (data not shown) is within its linear viscoelastic regime over the range of shear rates imposed. During the initial shear rate sweep, the nanocomposite is believed to change in two ways. First, the hypothesized mesoscale organoclay network is destroyed by stresses exceeding the inferred yield stress. Second, the highly anisotropic organoclay silicate layers and tactoids that comprise that network are oriented by the applied deformation to a degree that depends upon the magnitude of that deformation. Rheo-XRD studies by Lele et al. indicate that the two effects may be linked in that yielding appears to result from a small amount of flow-induced orientation sufficient to break the percolated network.[23]

The subsequent disorientation of organoclay domains and the resulting effect on rheological properties are also of interest. Hence, the presheared nanocomposite samples were annealed at 180 °C for 5−120 min, and the shear rate sweep was repeated. As observed in Figure 3, the low shear rate response is manifestly different from that of the initial sweep and minimally influenced by annealing time, at least over this limited range. After annealing for 5 min, the viscosity at the lowest shear rate remains half that of the initial sweep of as-processed material; moreover, after 120 min, the lowest shear rate viscosity is still substantially suppressed relative to the initial sweep. It is also noteworthy that the 5 min annealing data show the beginnings of a low shear rate plateau, although the divergent behavior gradually returns as the annealing time increases. Similar results (not shown) are observed for annealing at 210 °C.

Startup of Steady Shear. Figure 2 clearly demonstrates that the presence of organoclay profoundly alters the transient response of the nanocomposite to the startup of shear flow. Unlike the work of Solomon et al.,[21] however, which only presents data for organoclay disorientation following a flow-aligning shear, we seek to examine the influence of annealing time and temperature on the transient viscosity overshoot for both as-processed and presheared samples. In the data of Solomon et al., the transient overshoot for presheared samples continued to increase with annealing time over the course of 2000 s, but the relationship to the initial overshoot was not reported, and it is unclear for how long the magnitude of the overshoot would continue to increase. By including the as-processed material in the analysis, we are able to comment upon the morphological differences between as-processed and presheared samples. Furthermore, if the as-processed material is representative of an equilibrium, disordered state, including data for the overshoot associated with the initial deformation allows one to track the evolution of the material response back to that original disordered state.

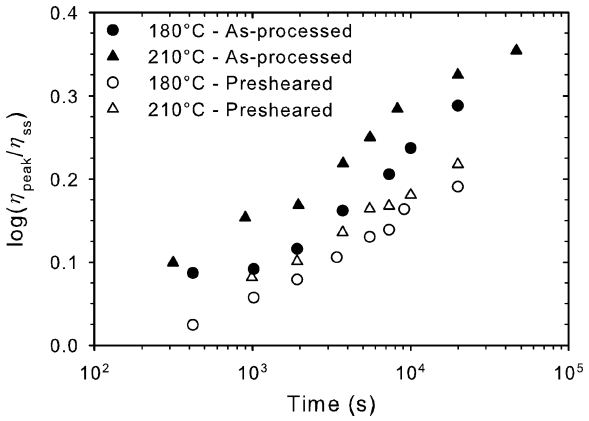

Figure 4. Plot of peak viscosity for overshoots scaled by the steady state viscosity in startup of shear flow experiments at a shear rate of 0.1 s^{-1}. As-processed samples were annealed for various times at either 180 or 210 °C prior to shear. Presheared samples were subjected to an initial shearing at 0.1 s^{-1} at 180°C for 5 min before annealing for various times at either 180 or 210 °C and subjected to shear in the reverse direction. In both cases, the shear for which data were recorded was performed at both 180 and 210 °C and the data averaged.

Since the salient feature of these transient startup responses is the overshoot in viscosity, we present the data as the ratio of the viscosity at the peak of the overshoot (η_{peak}) to the value at steady state (η_{ss}). The η_{peak}/η_{ss} results for as-processed and presheared (0.1 s^{-1}) samples are summarized in Figure 4 as a function of annealing time at both 180 and 210 °C. In all cases, the measured steady-state viscosity is consistent within 5% for every data point within a series, ensuring reasonable sample reproducibility and long-time thermo-oxidative stability.

It is immediately apparent that the organoclay morphology in both as-processed and presheared samples changes significantly during annealing, as evidenced by the large increases in the magnitude of the viscosity overshoots. The strong dependence on annealing time for the as-processed material clearly indicates that it is out-of-equilibrium after melt-blending. The reduced resistance to flow early in the annealing process points to a weaker mesoscale network that strengthens in time. Interestingly, at early times, temperature appears to play a modest role in distinguishing the two as-processed data sets, suggesting a thermally driven relaxation process at short annealing times. However, the rate at which the peak viscosity increases appears to be largely insensitive to temperature at longer annealing times, where the data are roughly parallel. Also noteworthy is the fact that the rate of increase in the peak viscosity slows somewhat after ~10 000 s.

The data in Figure 4 also demonstrate that the application of shear alters the development of the organoclay network as well. The steady shear rate sweeps presented in the previous section and by others show that shear in excess of the yield stress is effective at inducing orientation of anisotropic organoclay domains. Consequently, it is not unexpected to note that the magnitude of the viscosity overshoots for presheared samples is suppressed relative to as-processed samples, though the fact that such suppression spans the entire range of annealing times is surprising. Moreover, the rate at which the peak viscosity increases is also reduced relative to the as-processed samples and again shows minimal effect of temperature. Thus, it appears that the organoclay domains do not completely disorient following the deformation, at least on the time scale of the longest annealing time (6 h). Instead, they appear to re-network into an alternate configuration, perhaps rendered accessible by the shear and with residual orientation in the direction of flow. It should be emphasized, however, that even in this partially

flow-aligned state, the nanocomposite still exhibits substantial solidlike character relative to the matrix polymer, which fails to exhibit an overshoot at this shear rate.

SAOS. As mentioned previously, the terminal regime in SAOS has proven to be a sensitive probe of solidlike behavior in a broad spectrum of particle-filled polymeric liquids. In the case of organoclay-filled PP melts, the existence of a mesoscale organoclay network is of particular interest, and changes in such a network caused by flow or agglomeration due to weak attractive forces should alter the rheological signature at low frequency. Data for the storage modulus, loss tangent ($\tan \delta = G''/G'$), and complex viscosity ($|\eta^*| = \sqrt{(G'/\omega)^2+(G''/\omega)^2}$) will be primarily presented, since these parameters best reflect changes in the solidlike character of the samples over time.

Figure 5 shows results for (a) storage modulus, (b) loss modulus, and (c) loss tangent, where as-processed nanocomposite and matrix polymer samples have been subjected to consecutive SAOS sweeps (10−0.01 Hz) for up to 10 h. Time−temperature superposition (TTS) was performed at a reference temperature of 180 °C. First, while the polymer exhibits classic linear viscoelastic behavior, the nanocomposite sample shows distinct flattening of the storage modulus and decrease in the loss tangent in the terminal regime, signatures of solidlike behavior. It is well-known that low-frequency linear viscoelastic rheology is particularly sensitive to clay content, while the polymer matrix typically dominates the high-frequency response.[16,18,65] The latter is true here as well, as the nanocomposite and matrix polymer rheological properties are nearly coincident outside the terminal regime.

Additionally, the plots in Figure 5 clearly show transient buildup of solidlike character in the terminal regime for the nanocomposite in stark contrast to the data of Galgali et al.,[22] who reported a trend toward smaller values of storage and loss moduli (yet, inexplicably, an increase in zero-shear viscosity). With each consecutive SAOS sweep, the terminal values of the storage modulus and loss tangent shift to higher and lower values, respectively, whereas the polymer shows virtually no change. For the storage modulus, the increase in terminal values leads to a flattening of the curve and the reduced terminal slope observed by others;[13,16,23] however, such reports are typically for single SAOS sweeps and make no mention of time-dependent changes in the terminal response. The temperature dependence of the terminal response is also notable in that the curves at 180 and 210 °C differ from one another even in the initial frequency sweep. In principle, TTS should superpose the two curves unless temperature-dependent morphological changes are occurring during a characteristic frequency sweep. Since the frequency sweep is conducted from high to low values, the thermal history is sufficiently different by the time points in the terminal regime are acquired that TTS fails to superpose those data. It should also be noted that this increase in solidlike rheology is consistent with the increasing magnitude of the viscosity overshoots reported for the startup of shear flow in Figure 4.

The loss modulus data shown in Figure 5b are almost completely unaffected by annealing. Furthermore, the differences in the loss modulus for the nanocomposite and matrix polymer are minor, with the former exhibiting a flatter slope over the entire frequency range. Essentially, the organoclay has a negligible effect upon the viscous response of the material. As a result, it is apparent that the time-dependent behavior of the loss tangent stems almost entirely from the storage modulus. Again, these results contradict those of Galgali et al., who reported a decrease in the loss modulus for both compatibilized

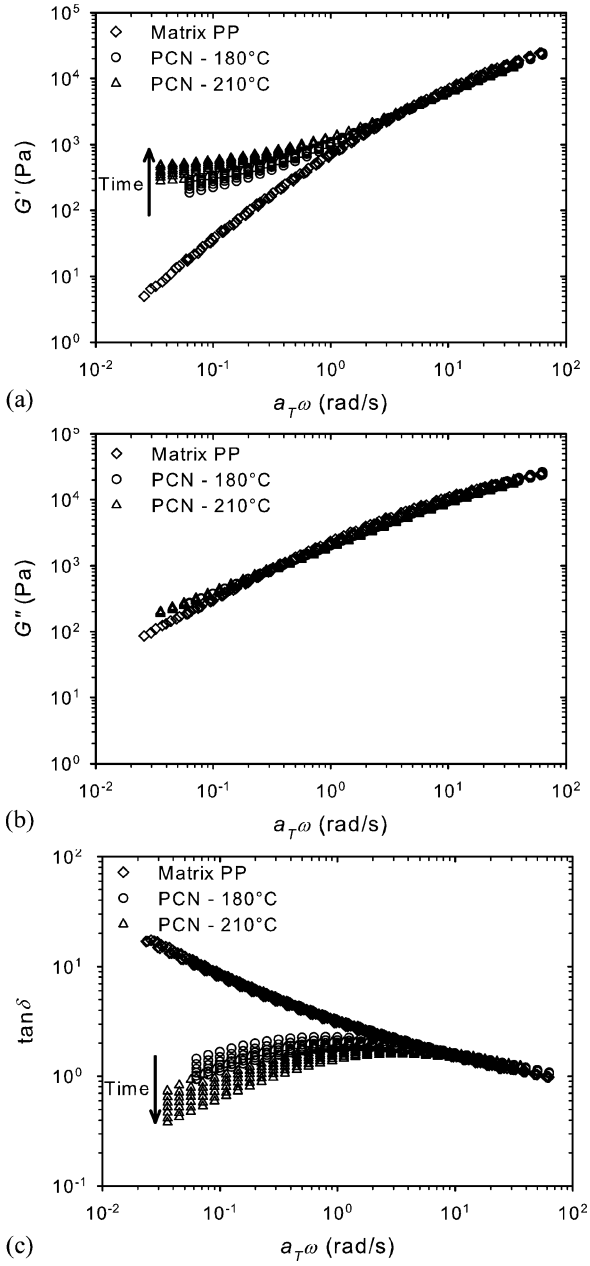

Figure 5. Plots of (a) storage modulus (G'), (b) loss modulus (G''), and (c) loss tangent ($\tan \delta$) vs shifted frequency for consecutive small-amplitude oscillatory shear (SAOS) sweeps performed at 180 and 210 °C for 10 h. Data are reported for the matrix polymer and as-processed 3 wt % nanocomposite. Time−temperature superposition is referenced to 180 °C.

and uncompatibilized 3 wt % nanocomposites.[22] In short, however, the as-processed nanocomposite used in these studies not only shows evidence of a percolated, solidlike network, but it is also becoming *increasingly* solidlike as it is annealed.

To more closely examine the time dependence of the terminal response for the as-processed nanocomposite, SAOS experiments were performed at a fixed frequency (0.01 Hz at 180 °C and 0.0147 Hz at 210 °C) for 9 h. Data for storage modulus, loss tangent, and complex viscosity are shown in Figure 6. First, a logarithmic dependence on time is observed for all three variables. The storage modulus, in particular, has been previously shown to scale logarithmically with time:

$$G' \sim t^{\beta} \tag{2}$$

where β varied between 0.1 and 0.25.[20] Here, at annealing times

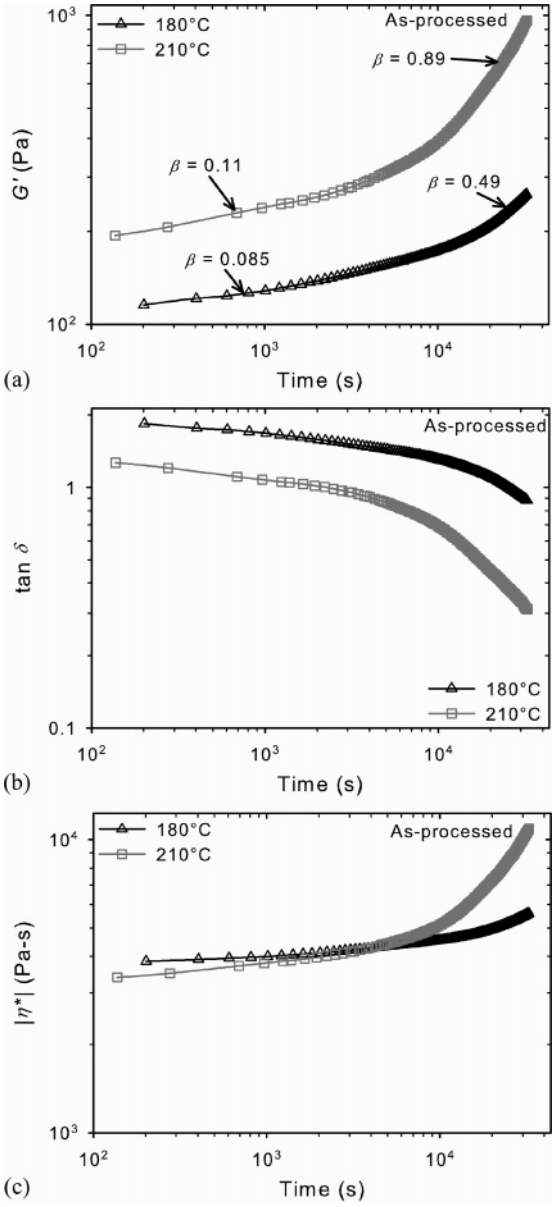

Figure 6. Plots of (a) storage modulus (G'), (b) loss tangent (tan δ), and (c) complex viscosity ($|\eta^*|$) vs annealing time for small-amplitude oscillatory shear of as-processed nanocomposite at 180 and 210 °C and fixed frequency of 0.01 and 0.0147 Hz, respectively.

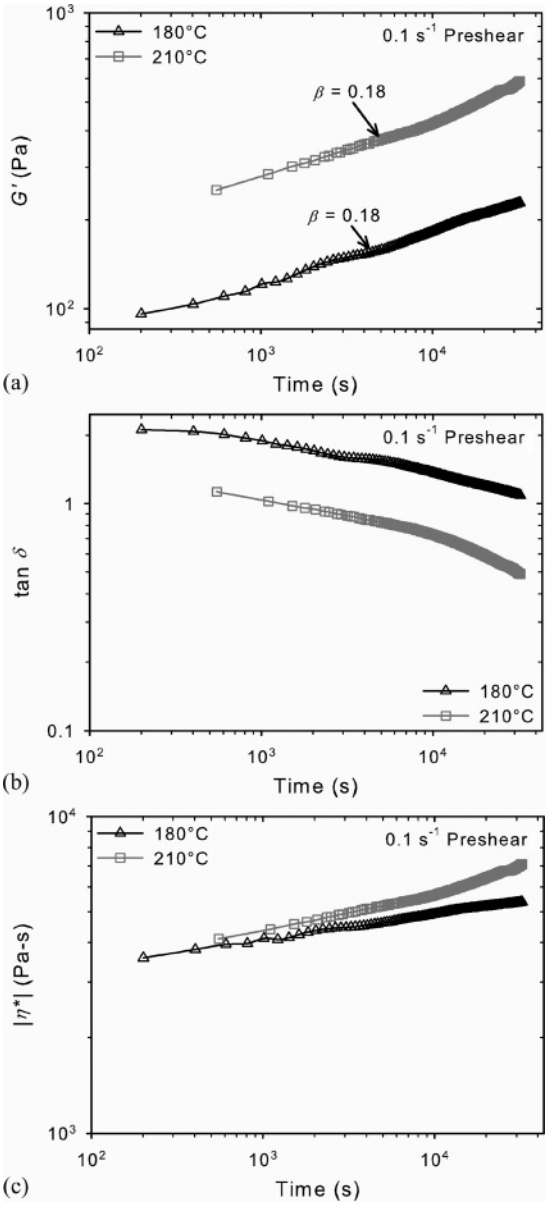

Figure 7. Plots of (a) storage modulus (G'), (b) loss tangent (tan δ), and (c) complex viscosity ($|\eta^*|$) vs annealing time for small-amplitude oscillatory shear of presheared nanocomposite at 180 and 210 °C and fixed frequency of 0.01 and 0.0147 Hz, respectively. Samples were presheared at a rate of 0.1 s^{-1} for 5 min prior to annealing.

up to ~3000 s, the curves at each temperature roughly parallel one another with slopes near 0.1. There is an initial offset in the storage modulus for the two temperatures that is also reflected in the loss tangent. Whether the offset is caused by differences in thermal history prior to the acquisition of the first data point or a general failure of TTS in the terminal regime is unclear. The offset is virtually absent for the complex viscosity in Figure 6c, making that parameter useful for studying the influence of thermal history. At longer annealing times, the effect of temperature becomes more pronounced, as the storage modulus and complex viscosity increase more precipitously and at earlier annealing times at 210 °C. The logarithmic scaling of storage modulus with time in this regime ($\beta = 0.49$ at 180 °C and 0.89 at 210 °C) is substantially stronger than that reported by Ren et al. Hence, in contrast to the startup flow data, the annealing temperature markedly affects the time-dependent buildup of solidlike character. The significant change in the logarithmic dependence with time is also indicative of a two-stage process of network formation during annealing.

The earlier data for startup of shear flow indicate that anisotropic organoclay domains are flow-aligned at these shear rates. The yielding of the hypothesized mesoscale organoclay network and concomitant flow-aligning of its constituent elements should be reflected in the linear viscoelastic response. Hence, similar SAOS experiments at fixed frequency were conducted on samples presheared at 0.1 and 0.5 s^{-1} for 5 min prior to annealing. These data are presented in Figures 7 and 8, respectively, where the focus is now upon the influence of thermal and deformation history on the time-dependent terminal behavior. Considering thermal history first, qualitatively similar responses are observed for presheared and as-processed samples. The storage modulus, loss tangent, and complex viscosity all show logarithmic time dependence, becoming increasingly solidlike with time. The logarithmic scaling of the storage modulus in Figures 7a and 8a are consistent with the range observed by Ren et al. and largely insensitive to the annealing temperature. In fact, with the exception of an offset in the storage

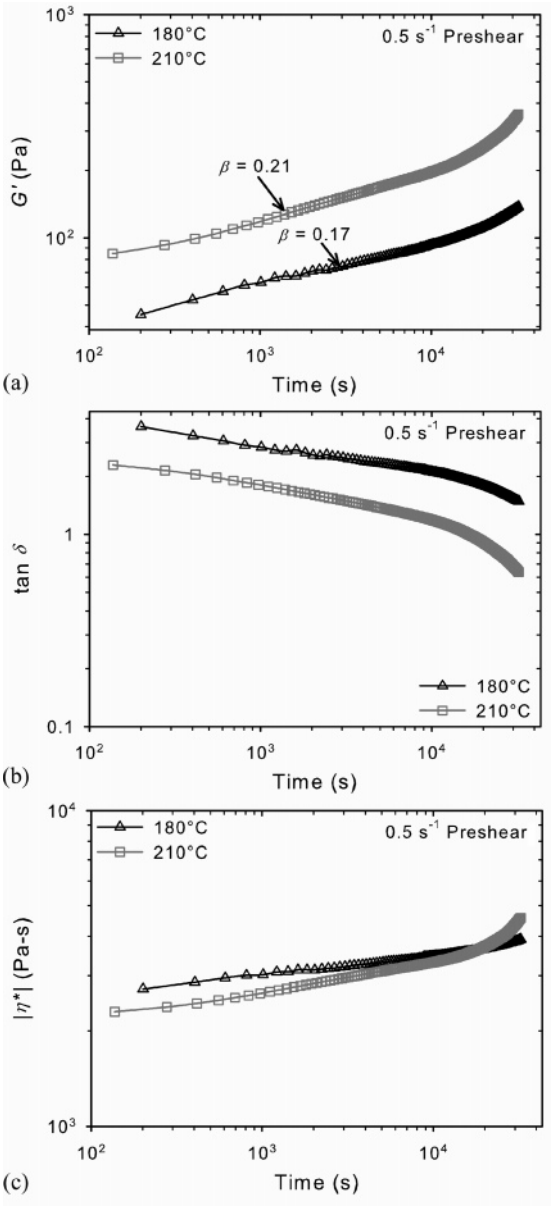

Figure 8. Plots of (a) storage modulus (G'), (b) loss tangent (tan δ), and (c) complex viscosity ($|\eta^*|$) vs annealing time for small-amplitude oscillatory shear of presheared nanocomposite at 180 and 210 °C and fixed frequency of 0.01 and 0.0147 Hz, respectively. Samples were presheared at a rate of 0.5 s^{-1} for 5 min prior to annealing.

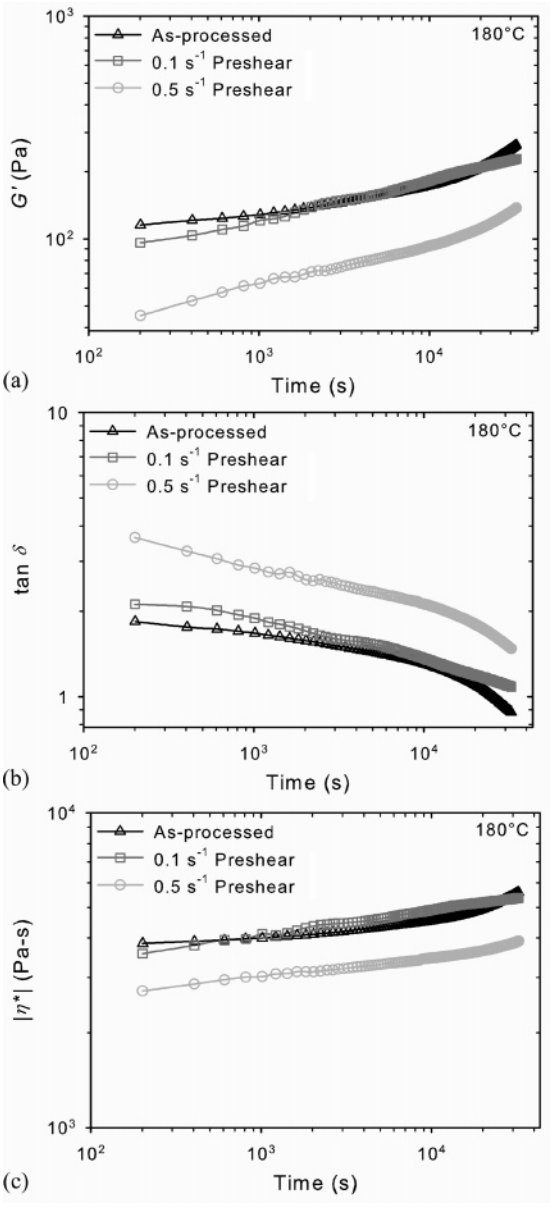

Figure 9. Plots of (a) storage modulus (G'), (b) loss tangent (tan δ), and (c) complex viscosity ($|\eta^*|$) vs annealing time for small-amplitude oscillatory shear of the nanocomposite at 180 °C and fixed frequency of 0.01 Hz. The data contrast the increase in solidlike behavior for as-processed and presheared samples. Presheared samples were subjected to a shear rate of 0.1 or 0.5 s^{-1} for 5 min prior to annealing.

modulus and loss tangent, the data for the 0.1 s^{-1} presheared sample at the two temperatures are virtually indistinguishable. The complex viscosity, however, offers the best comparison since the offset between the two curves is minimal. Like the as-processed results in Figure 6c, the complex viscosity for both presheared samples at 210 °C increases more steeply after ~10 000 s. While delayed in its effect relative to the as-processed material, temperature becomes important at long annealing times in the presheared samples as well.

The data from Figures 6−8 are replotted in Figures 9 and 10 such that the influence of deformation history may be isolated at 180 and 210 °C, respectively. At both temperatures, preshearing at 0.1 s^{-1} appears to have only a nominal effect over most of the sampling period. The results at 180 °C (see Figure 9) are particularly striking, as the storage modulus, loss tangent, and complex viscosity curves for as-processed and 0.1 s^{-1} presheared samples track one another very closely. Only at very long annealing time do the curves begin to diverge, suggesting that the microstructural evolution responsible for the solidlike buildup has been subtly altered by the preshearing. The effect is more visible at 210 °C (Figure 10), where the kinetics of the solidlike buildup are accelerated relative to 180 °C at long annealing times. However, the development of solidlike terminal behavior in the sample presheared at 0.1 s^{-1} is suppressed relative to the as-processed sample, pointing to a somewhat weaker mesoscopic network.

Preshearing at a higher shear rate (0.5 s^{-1}) alters the subsequent linear viscoelastic response much more profoundly. The reduction in storage modulus and complex viscosity and increase in loss tangent over the entire annealing period all point to a more liquidlike sample and a weakened network. Interestingly, the increase in solidlike behavior with annealing time for the 0.5 s^{-1} presheared sample occurs at a rate similar to that for both the 0.1 s^{-1} presheared and as-processed samples, judging from the parallel curves in Figures 9 and 10. Only at

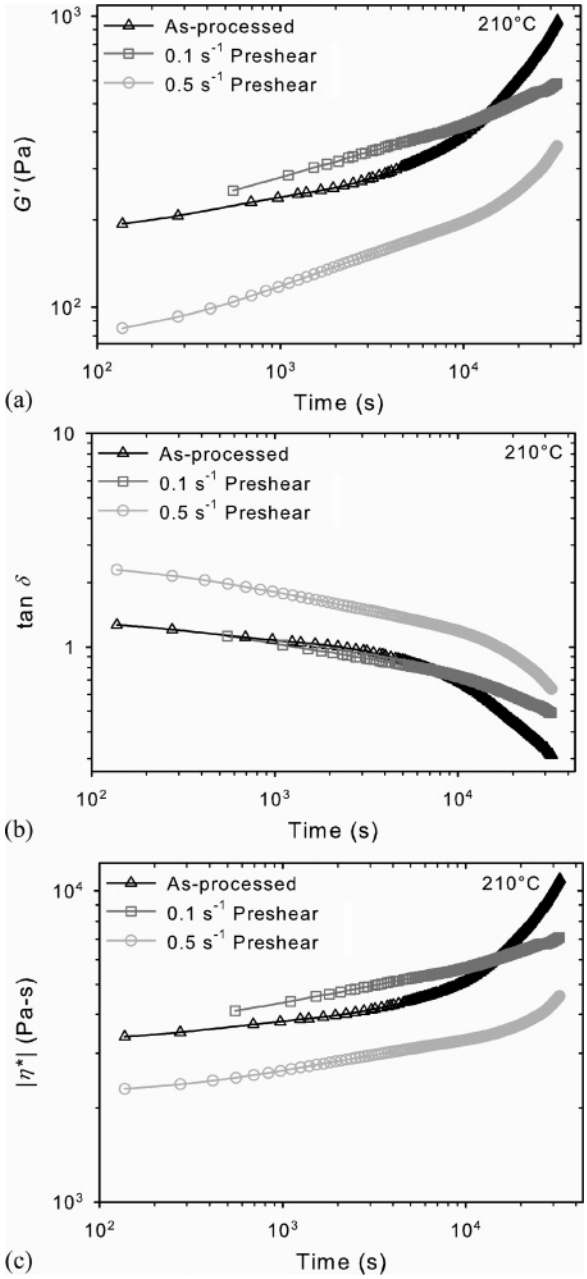

Figure 10. Plots of (a) storage modulus (G'), (b) loss tangent (tan δ), and (c) complex viscosity ($|\eta^*|$) vs annealing time for small-amplitude oscillatory shear of the nanocomposite at 210 °C and fixed frequency of 0.0147 Hz. The data contrast the increase in solidlike behavior for as-processed and presheared samples. Presheared samples were subjected to a shear rate of 0.1 or 0.5 s^{-1} for 5 min prior to annealing.

the end of the 9 h annealing period do the slopes of the 0.5 s^{-1} curves become steeper than those for 0.1 s^{-1}, a result that is particularly evident at 210 °C. It has been explained in prior work that the flow alignment of organoclay domains reduces the effective clay−clay interaction and its contribution to the viscoelastic response, resulting in interactions that occur in a more two- than three-dimensional fashion.[14,18] Our results qualitatively support this hypothesis, as the stronger deformation clearly leads to more liquidlike behavior.

IV. Discussion

In order to frame the discussion of these data, it is constructive to first enumerate characteristics of PCNs established by this and other studies:

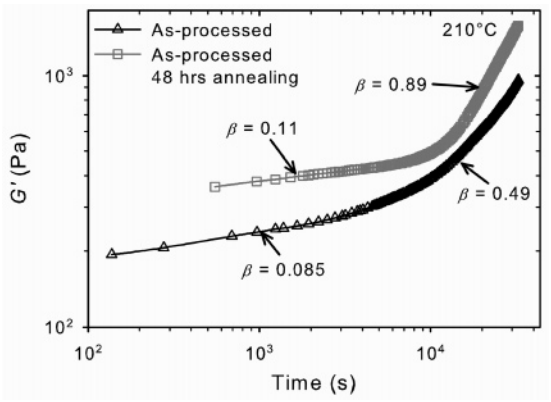

Figure 11. Plot of storage modulus (G') vs annealing time for small-amplitude oscillatory shear of the nanocomposite at 210 °C and fixed frequency of 0.0147 Hz. Data show that a nanocomposite sample annealed for 48 h at 180 °C in a vacuum oven prior to experimentation is initially more solidlike than as-processed material, and solidlike behavior builds rapidly at earlier times.

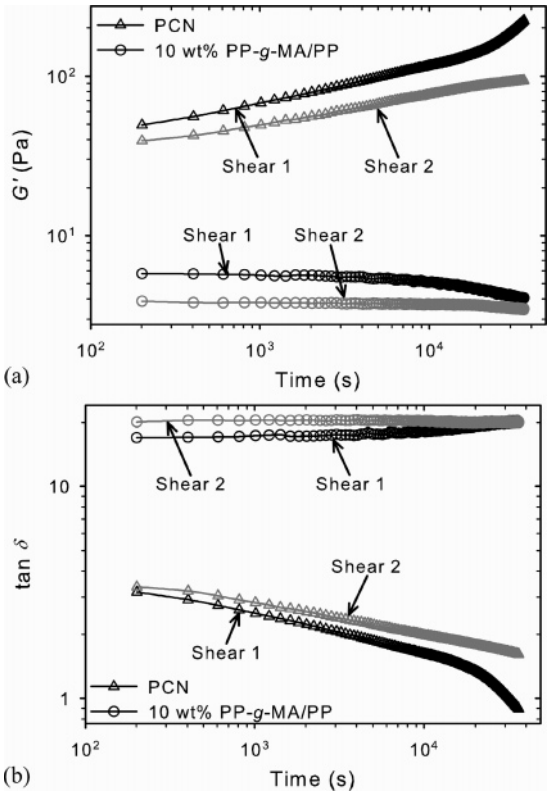

Figure 12. Plots of (a) storage modulus (G') and (b) loss tangent (tan δ) vs annealing time for small-amplitude oscillatory shear of the nanocomposite and 10 wt % PP-*g*-MA/PP samples at 180 °C and fixed frequency of 0.01 Hz. Each sample was presheared at a rate of 0.5 s^{-1} for 5 min prior to annealing for 11 h ("Shear 1") and then sheared a second time at 0.5 s^{-1} for 5 min before annealing again for 11 h ("Shear 2").

- The overshoot in viscosity (or shear stress) in startup of shear flow is a purely hydrodynamic response caused by the flow-induced orientation of organoclay domains, and Brownian relaxation processes do not play a significant role in the rheological response. The occurrence of the overshoot peak at constant strain, independent of shear rate,[21] and the constant TTS shift factors for matrix polymer and nanocomposites[18,21] support this notion.
- The solidlike rheological response of the nanocomposite in the terminal regime does not stem from confinement of polymer chains, as the flow activation energy of nanocomposites is the

same as that of the matrix polymer. Rather, frictional clay−clay interactions are the more likely source of solidlike behavior.[22]

- Yield behavior indicates that the nanocomposite microstructure is characterized by a percolated three-dimensional network of organoclay domains, which include individual silicate layers and tactoids.[18,20] Imposing stresses in excess of the yield stress ruptures the network and tends to orient the anisotropic organoclay domains.[23]
- Both as-processed nanocomposite directly from a twin-screw extruder and nanocomposite subjected to a controlled thermal and deformation history are out-of-equilibrium and characterized by macroscopic material properties (e.g., storage modulus, complex viscosity) that grow logarithmically in time during annealing above the melt temperature of the polymer. Such behavior is analogous to the soft glassy dynamics (or physical aging) observed in a variety of material systems.
- Following a deformation in excess of the yield stress, the disorientation of flow-aligned organoclay domains may be arrested prematurely,[20] as evidenced by the divergence of the as-processed and presheared curves for peak viscosity in startup of shear flow and storage modulus (and complex viscosity) in SAOS.

Central to a discussion of PCN morphology is the idea of an organoclay network at filler concentrations above the mechanical percolation threshold. Depending upon the degree of exfoliation, mechanical percolation of PCNs tends to occur at a few wt %. The mesoscale structure of the network itself, however, is unclear. The experiments described herein suggest that the network continues to evolve in time for both as-processed and presheared samples, rendering the notion of an equilibrium state for these materials arguable. In fact, one important question is how long the buildup of the solidlike network continues during annealing. To address that question, a nanocomposite sample was annealed in a vacuum oven at 180 °C for 48 h before being transferred to the rheometer and subjected to SAOS at 210 °C for 9 h. Data for the storage modulus are compared with those for as-processed nanocomposite annealed at 210 °C in Figure 11. The sample has clearly become more solidlike during vacuum oven annealing, as evidenced by the substantially higher initial storage modulus and smaller loss tangent (data not shown). For the first 3000 s, however, the logarithmic dependence of the two samples is similar. Upon further annealing at 210 °C, both samples continue to become more solidlike, although the storage modulus of the vacuum oven annealed sample increases more steeply than that of the standard as-processed sample. Thus, the buildup of the solidlike network seemingly begins in the vacuum oven and continues unabated in the rheometer.

A second question concerns the lability of the network upon imposition of shear. Figure 12 shows two sets of SAOS data for the PCN sample as well as a blend of 10 wt % PP-*g*-MA and PP base resin in the absence of organoclay (designated 10 wt % PP-*g*-MA/PP). Samples of each were first compression molded, annealed at 210 °C for 10 min, sheared at a rate of 0.5 s^{-1} for 5 min at 180 °C, and subjected to SAOS at a fixed frequency of 0.01 Hz for 11 h as the presumed organoclay network developed. These data are labeled "Shear 1". At the end of 11 h, the same samples were again sheared at a rate of 0.5 s^{-1} for 5 min to eradicate the network, after which the network was again allowed to build for 11 h during SAOS at 0.01 Hz (data denoted as "Shear 2"). The logarithmic time dependence of the storage modulus following the initial deformation of the PCN sample resembles the identical experiment reported in Figure 8a. Following the second deformation, the storage modulus drops to a value comparable to that after the first deformation (though lower due to some thermo-oxidative degradation of the PP matrix), demonstrating the reversibility of the network formation process. The logarithmic growth of the storage modulus then begins anew, since the curve roughly parallels the initial storage modulus data. The only deviation comes at long times, where the late-stage upturn in the time dependence is not observed for the "Shear 2" data. Whether this change in the long-time behavior is due to differences in the organoclay microstructure between the first and second deformations is currently being studied. Companion data for the loss tangent are also provided in Figure 12b for completeness.

The results for the 10 wt % PP-*g*-MA/PP blend in Figure 12 reveal that the presence of the PP-*g*-MA does not explicitly contribute to the logarithmic increases in storage modulus over time. Following both deformations, the storage modulus gradually *decreases* with time, which reflects modest thermo-oxidative degradation. Moreover, the initial value of the storage modulus after the second deformation is identical to that at the end of the 11 h period following the first deformation, indicating the absence of structure. The conclusion is important, as previous work with pure maleated polyethylene (PE-*g*-MA) compatibilizer samples showed significant logarithmic increases in storage and loss moduli over a period of 1 h.[66] These results were attributed to dipole−dipole and hydrogen-bonding interactions between pendant succinic anhydride and succinic acid functionalities, which were presumed to drive the formation of a reversible, labile network. While similar behavior is undoubtedly relevant to PP-*g*-MA in its pure form as well, its dilution in the matrix PP at the concentration studied here appears to diminish or eliminate the effect. Hence, the presence of organoclay is essential to the logarithmic time-dependent rheology.

Galgali et al. conducted XRD scans of PP−clay nanocomposites and reported a shifting of the basal spacing (silicate layer thickness plus intergallery distance) to smaller values accompanied by a broadening of the peak and a decrease in peak intensity.[22] The decrease in basal spacing was attributed to surfactant degradation, which for the quaternary alkylammonium surfactants is known to occur above 200 °C.[67,68] However, the authors suggested that exfoliation of layers from the end of tactoid stacks during annealing could account for the peak broadening and reduction in peak intensity. If true, continued exfoliation during annealing would lead to more numerous (if slightly thinner) organoclay domains and increasingly solidlike behavior in the nanocomposite. To examine this possibility, XRD scans of as-processed nanocomposite and samples annealed for 10 h at 180 and 210 °C were performed. These results are shown in Figure 13, along with the scan for the dry clay as a reference. The result labeled "PCN—As-processed" is derived from the same sample as the TEM image presented in Figure 1. The basal spacing for the as-processed nanocomposite increases modestly relative to the dry clay, demonstrating the ability of PP-*g*-MA compatibilizer to intercalate between silicate layers during melt-blending. As the sample is annealed, however, the basal spacing decreases, presumably due to surfactant degradation since the shift is more pronounced at 210 °C. Additionally, the peaks broaden and diminish in intensity, as observed by Galgali et al., particularly at the higher temperature.

Taken in isolation, these results support the idea that continued exfoliation during annealing is responsible for the increasingly solidlike rheology. However, in the absence of shear, such exfoliation requires the presence of PP-*g*-MA

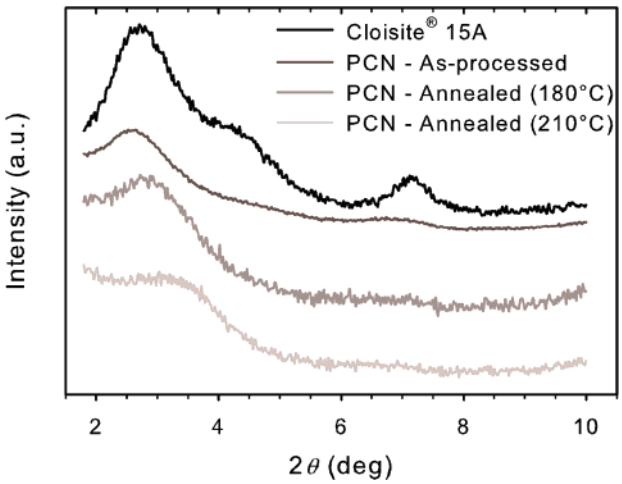

Figure 13. XRD scans of dry Cloisite 15A clay, as-processed nanocomposite, and as-processed nanocomposite annealed for 10 h at 180 or 210 °C. Basal spacing for the annealed samples decreases slightly, likely due to surfactant degradation. The peak at 210 °C broadens and diminishes in height, though continued exfoliation of organoclay during annealing is unlikely.

compatibilizer, since the interaction between PP and organoclay is thermodynamically unfavorable. A separate experimental study examining the influence of compatibilizer on the time-dependent network formation of PCNs is in progress, the details of which will be reported elsewhere.[69] Importantly, another PP−clay nanocomposite containing 3 wt % clay but no PP-*g*-MA was studied in SAOS as previously described. Although a frequency sweep revealed the same liquidlike terminal behavior as the matrix polymer, SAOS experiments at fixed low frequency also showed a slow solidlike buildup during annealing. As a result, it is highly unlikely that the development of the solidlike network is due to exfoliation during annealing. This result serves two purposes. First, it demonstrates that, while PP-*g*-MA unequivocally improves exfoliation during melt-blending, neither it nor mechanical percolation is required to observe time-dependent increases in storage modulus and solidlike behavior. Second, it reinforces the notion that intermolecular associations of succinic anhydride and succinic acid functionalities present in PP-*g*-MA are not responsible for the time-dependent rheology as they are in samples of pure PE-*g*-MA.[66] The observed peak broadening and reduction in intensity in XRD of annealed samples undoubtedly stem from causes other than continued exfoliation. Like samples used in XRD of nearly all other studies of PCNs, the samples studied here were compression-molded and thus subjected to a modest squeezing flow, which tends to flow-align organoclay domains in the radial direction. This high degree of orientation would lead to a strong XRD signal in unannealed samples, since the number of diffraction events would be large. By contrast, the organoclay disorientation that occurs during annealing would increase the number of domains tilted out-of-plane relative to the incident X-ray beam, reducing signal intensity and broadening the peak. Consequently, we ascribe the changes in signal intensity to this effect and suggest that sample preparation is of paramount importance in the discussion of these XRD scans and those of other researchers.

We turn again to the fundamental interest in the microstructural transformations responsible for the time-dependent behavior captured by these rheological experiments. Similar behavior has been observed following the flow alignment of organoclay-filled polymers other than PP, including PS and PS−PIB block copolymers,[20] despite the fact that the thermodynamic interaction between those polymers and organoclay is quite different than it is for PP. Thus, it is tempting to ascribe a universal mechanism to the phenomenon; however, the time-dependent rheology may derive from entirely different microstructural changes that may, in fact, depend upon the interaction between the polymer and the clay. Aqueous Laponite dispersions offer an apt analogy. Adjusting the ionic strength tunes the attractive and repulsive forces between clay particles and dictates whether the material is classified as a repulsive ("Wigner") colloidal glass, an attractive glass, or a gel.[70] All three systems exhibit similar dynamical rheological behavior,[71] referred to as *aging* for glasses and *gelation* for gels, but more broadly referred to as soft glassy dynamics.[47,72] Among their common traits is the logarithmic dependence of storage modulus and complex viscosity with time. At the same time, these systems have quite different structural organization. For example, a glass is homogeneous on interparticle distances with elasticity derived from caging effects,[73] while a gel possesses a hierarchical structure with elasticity caused by a percolated infinite network that is inhomogeneous on the length scale of the entire network.[74] Despite the manifold differences in network structure, however, it is not always easy to experimentally detect the differences between a glass and a gel except in the extreme limits of ionic strength.[75] In any event, like the ionic strength for these dispersions, the relative attraction between the host polymer and the organoclay may alter the physics of microstructural change in PCNs.

In PP−clay nanocomposites, long-range repulsive interactions are negated by the presence of cationic surfactant, leaving short-range attractive van der Waals forces as the primary driving force for microstructural change. As a result, the sample discussed here is most similar to attractive colloidal gels. Solomon et al. argued that PP−clay nanocomposites possess the structural hierarchy characteristic of colloidal gels.[21] They suggested that individual platelets and tactoids aggregate into larger organoclay domains that assemble into a volume-spanning, heterogeneous organoclay network as a result of attractive interactions. Accepting this physical picture permits a plausible reference frame for interpreting the experimental data described previously.

The startup of shear and SAOS experiments each offer insight into the observed microstructural changes. Since the viscosity overshoots are strictly a hydrodynamic response, the startup experiments are particularly sensitive to the disorientation kinetics of flow-aligned platelets and tactoids, the constitutive elements of the proposed gel-like network. Returning then to the viscosity overshoot data in Figure 4, the most striking feature is the divergence of the as-processed and pressheared data. We believe that flow ruptures the gel-like network present in the as-processed material and flow-aligns organoclay domains to a degree that depends upon the magnitude of the deformation, consistent with the rheo-XRD experiments of Lele et al.[23] The subsequent re-formation of the organoclay network should then be governed by the simultaneous disorientation and assembly of organoclay domains into a mesoscale network. We have already argued that Brownian motion is not important to the rheological response in startup flow; however, it is useful to obtain an order of magnitude estimate of the rotational diffusivity (D_{r0}) of organoclay platelets or tactoids (treating them as comparable to one another) in order to assess the time scale for Brownian motion to disorient organoclay domains. Thus, we apply the formula for a circular disk of diameter d[19]

$$D_{r0} = \frac{3k_B T}{4\eta_0 d^3} \tag{3}$$

where η_0 is the polymer matrix viscosity, and conclude that the time scale for rotational Brownian motion is larger than the time scale of these experiments and an unlikely driving force for microstructural change. The attractive van der Waals forces motivating the formation of the organoclay network is a more probable cause of platelet and tactoid disorientation. For the presheared samples, however, that disorientation process may be prematurely arrested by the formation of the larger network assembly, thereby trapping organoclay domains in a metastable, partially oriented state.

This hypothesis is also consistent with the SAOS data presented in Figures 6−10. The material response to SAOS is particularly sensitive the formation of the solidlike network. For both as-processed and presheared samples, the logarithmic time dependence of the rheological functions is small, nearly constant, and only modestly sensitive to temperature and deformation history for approximately the first 10 000 s of annealing. At longer annealing times, the logarithmic time dependence becomes substantially stronger, particularly for the as-processed sample, and temperature plays a more prominent role in controlling the time at which the scaling transition occurs. We suggest that this transition denotes a shift in importance from the disorientation of platelets and tactoids to the assembly of organoclay domains into a growing heterogeneous, gel-like network being dominant. The increased role of temperature suggests that a decreased polymer matrix viscosity at higher temperature may accelerate the formation of the network. Additionally, the flow-induced alignment of organoclay domains seems to suppress the rheological sensitivity to network formation (see Figure 10 in particular), although it is possible that a network of organoclay domains with preferred orientation in the direction of shear may have a weaker rheological signature.

V. Conclusions

In summary, a systematic approach has been used to study the time-dependent buildup of solidlike rheological behavior in a compatibilized 3 wt % PP−clay nanocomposite. Although rheology is only an indirect probe of microstructure, it is sensitive to changes in the orientation state of organoclay domains as well as the proposed gel-like, mesoscale organoclay network. Steady shear rate sweeps revealed that high shear rates flow-align organoclay domains, which subsequently fail to disorient significantly after annealing for 2 h. Startup of steady shear flow and SAOS experiments demonstrated that even the as-processed material is inherently out-of-equilibrium, exhibiting annealing time-dependent viscosity overshoots and logarithmic growth of rheological functions with time indicative of an increasingly solidlike material. The logarithmic growth with time in SAOS is relatively weak and largely independent of temperature at shorter annealing times but substantially stronger and dependent on temperature at longer annealing times. Samples subjected to preshearing show similar logarithmic dependence with time, although the onset of stronger growth appears to be suppressed by incomplete disorientation of flow-aligned organoclay domains. The rheological behavior, which mimics the soft glassy dynamical response characteristic of attractive colloidal dispersions and other materials, is indicative of the formation of a gel-like organoclay network prior to the complete disorientation of organoclay domains. Further studies utilizing techniques capable of directly imaging the mesoscale network structure would be of great value in further illuminating the physics behind the time-dependent rheology described herein.

Acknowledgment. The authors thank Dr. Robert Sammler of The Dow Chemical Co. and Dr. Leigh Allen of Crompton Corp. for the generous donation of the H700-12 polypropylene resin and Polybond 3200 PP-*g*-MA compatibilizer, respectively. We further acknowledge the assistance of Andrew Yacykewych of C.W. Brabender Instruments, Inc., in melt-blending the nanocomposite sample. We are also appreciative of numerous enlightening discussions with Prof. Ramanan Krishnamoorti. Finally, we gratefully recognize the financial support of the National Science Foundation (NSF CAREER Award CTS-0134275).

References and Notes

(1) Usuki, A.; Kawasumi, M.; Kojima, Y.; Okada, A.; Kurauchi, T.; Kamigaito, O. *J. Mater. Res.* **1993**, *8*, 1174−1178.
(2) Usuki, A.; Kojima, Y.; Kawasumi, M.; Okada, A.; Fukushima, Y.; Kurauchi, T.; Kamigaito, O. *J. Mater. Res.* **1993**, *8*, 1179−1184.
(3) Kojima, Y.; Usuki, A.; Kawasumi, M.; Okada, A.; Fukushima, Y.; Kurauchi, T.; Kamigaito, O. *J. Mater. Res.* **1993**, *8*, 1185−1189.
(4) Lan, T.; Pinnavaia, T. J. *Chem. Mater.* **1994**, *6*, 2216−2219.
(5) Messersmith, P. B.; Giannelis, E. P. *J. Polym. Sci., Part A: Polym. Chem.* **1995**, *33*, 1047−1057.
(6) Gilman, J. W.; Jackson, C. L.; Morgan, A. B.; Harris, R.; Manias, E.; Giannelis, E. P.; Wuthenow, M.; Hilton, D.; Phillips, S. H. *Chem. Mater.* **2000**, *12*, 1866−1873.
(7) Ray, S. S.; Okamoto, M. *Prog. Polym. Sci.* **2003**, *28*, 1539−1641.
(8) Marchant, D.; Jayaraman, K. *Ind. Eng. Chem. Res.* **2002**, *41*, 6402−6408.
(9) Cho, J. W.; Paul, D. R. *Polymer* **2001**, *42*, 1083−1094.
(10) Dennis, H. R.; Hunter, D. L.; Chang, D.; Kim, S.; White, J. L.; Cho, J. W.; Paul, D. R. *Polymer* **2001**, *42*, 9513−9522.
(11) Homminga, D.; Goderis, B.; Hoffman, S.; Reynaers, H.; Groeninckx, G. *Polymer* **2005**, *46*, 9941−9954.
(12) Khan, S. A.; Prud'homme, R. K. *Rev. Chem. Eng.* **1987**, *4*, 205−270.
(13) Krishnamoorti, R.; Giannelis, E. P. *Macromolecules* **1997**, *30*, 4097−4102.
(14) Krishnamoorti, R.; Ren, J.; Silva, A. S. *J. Chem. Phys.* **2001**, *114*, 4968−4973.
(15) Krishnamoorti, R.; Yurekli, K. *Curr. Opin. Colloid Interface Sci.* **2001**, *6*, 464−470.
(16) Lim, Y. T.; Park, O. O. *Rheol. Acta* **2001**, *40*, 220−229.
(17) Lim, S. T.; Lee, C. H.; Choi, H. J.; Jhon, M. S. *J. Polym. Sci., Part B: Polym. Phys.* **2003**, *41*, 2052−2061.
(18) Ren, J. X.; Silva, A. S.; Krishnamoorti, R. *Macromolecules* **2000**, *33*, 3739−3746.
(19) Ren, J. X.; Krishnamoorti, R. *Macromolecules* **2003**, *36*, 4443−4451.
(20) Ren, J. X.; Casanueva, B. F.; Mitchell, C. A.; Krishnamoorti, R. *Macromolecules* **2003**, *36*, 4188−4194.
(21) Solomon, M. J.; Almusallam, A. S.; Seefeldt, K. F.; Somwangthanaroj, A.; Varadan, P. *Macromolecules* **2001**, *34*, 1864−1872.
(22) Galgali, G.; Ramesh, C.; Lele, A. *Macromolecules* **2001**, *34*, 852−858.
(23) Lele, A.; Mackley, M.; Galgali, G.; Ramesh, C. *J. Rheol.* **2002**, *46*, 1091−1110.
(24) Hoffmann, B.; Dietrich, C.; Thomann, R.; Friedrich, C.; Mulhaupt, R. *Macromol. Rapid Commun.* **2000**, *21*, 57−61.
(25) Fornes, T. D.; Yoon, P. J.; Keskkula, H.; Paul, D. R. *Polymer* **2001**, *42*, 9929−9940.
(26) Li, J.; Zhou, C. X.; Wang, G.; Zhao, D. L. *J. Appl. Polym. Sci.* **2003**, *89*, 3609−3617.
(27) Gu, S. Y.; Ren, J.; Wang, Q. F. *J. Appl. Polym. Sci.* **2004**, *91*, 2427−2434.
(28) Lertwilmolnun, W.; Vergnes, B. *Polymer* **2005**, *46*, 3462−3471.
(29) Meincke, O.; Hoffmann, B.; Dietrich, C.; Friedrich, C. *Macromol. Chem. Phys.* **2003**, *204*, 823−830.
(30) Sohn, J. I.; Lee, C. H.; Lim, S. T.; Kim, T. H.; Choi, H. J.; Jhon, M. S. *J. Mater. Sci.* **2003**, *38*, 1849−1852.
(31) Zhao, J.; Morgan, A. B.; Harris, J. D. *Polymer* **2005**, *46*, 8641−8660.
(32) Giannelis, E. P.; Krishnamoorti, R.; Manias, E. *Adv. Polym. Sci.* **1999**, *138*, 107−147.
(33) Maiti, P. *Langmuir* **2003**, *19*, 5502−5510.
(34) Mitchell, C. A.; Krishnamoorti, R. *J. Polym. Sci., Part B: Polym. Phys.* **2002**, *40*, 1434−1443.
(35) Lobe, V. M.; White, J. L. *Polym. Eng. Sci.* **1979**, *19*, 617−624.
(36) White, J. L.; Tanaka, H. *J. Appl. Polym. Sci.* **1981**, *26*, 579−589.
(37) Suetsugu, Y.; White, J. L. *J. Appl. Polym. Sci.* **1983**, *28*, 1481−1501.
(38) Suh, C. H.; White, J. L. *J. Non-Newtonian Fluid Mech.* **1996**, *62*, 175−206.

(39) Luckham, P. F.; Rossi, S. *Adv. Colloid Interface Sci.* **1999**, *82*, 43−92.
(40) Jogun, S. M.; Zukoski, C. F. *J. Rheol.* **1999**, *43*, 847−871.
(41) Cocard, S.; Tassin, J. F.; Nicolai, T. *J. Rheol.* **2000**, *44*, 585−594.
(42) Willenbacher, N. *J. Colloid Interface Sci.* **1996**, *182*, 501−510.
(43) Abou, B.; Bonn, D.; Meunier, J. *Phys. Rev. E* **2001**, *64*, 021510.
(44) Bonn, D.; Tanase, S.; Abou, B.; Tanaka, H.; Meunier, J. *Phys. Rev. Lett.* **2002**, *89*, 015701.
(45) Bellour, M.; Knaebel, A.; Harden, J. L.; Lequeux, F.; Munch, J. P. *Phys. Rev. E* **2003**, *67*, 031405.
(46) Cipelletti, L.; Ramos, L. *J. Phys.: Condens. Matter* **2005**, *17*, R253−R285.
(47) Sollich, P.; Lequeux, F.; Hebraud, P.; Cates, M. E. *Phys. Rev. Lett.* **1997**, *78*, 2020−2023.
(48) Fielding, S. M.; Sollich, P.; Cates, M. E. *J. Rheol.* **2000**, *44*, 323−369.
(49) Liu, A. J.; Nagel, S. R. *Nature* **1998**, *396*, 21−22.
(50) Ozon, F.; Narita, T.; Knaebel, A.; Debregeas, G.; Hebraud, P.; Munch, J. P. *Phys. Rev. E* **2003**, *68*.
(51) Krishnamoorti, R.; Vaia, R. A.; Giannelis, E. P. *Chem. Mater.* **1996**, *8*, 1728−1734.
(52) Walker, L. M.; Mortier, M.; Moldenaers, P. *J. Rheol.* **1996**, *40*, 967−981.
(53) Maffettone, P. L.; Marrucci, G.; Mortier, M.; Moldenaers, P.; Mewis, J. *J. Chem. Phys.* **1994**, *100*, 7736−7743.
(54) Beekmans, F.; Gotsis, A. D.; Norder, B. *J. Rheol.* **1996**, *40*, 947−966.
(55) Caputo, F. E.; Burghardt, W. R.; Berret, J. F. *J. Rheol.* **1999**, *43*, 765−779.
(56) Caputo, F. E.; Burghardt, W. R. *Macromolecules* **2001**, *34*, 6684−6694.
(57) Pignon, F.; Magnin, A.; Piau, J. M.; Fuller, G. G. *J. Rheol.* **2003**, *47*, 371−388.
(58) Guido, S.; Minale, M.; Maffettone, P. L. *J. Rheol.* **2000**, *44*, 1385−1399.
(59) Van Puyvelde, P.; Moldenaers, P. *Proc. XIIIth Int. Congr. Rheol.* **2000**, *3*, 134−136.
(60) Chen, S.; Phan-Thien, N.; Fan, X. J.; Khoo, B. C. *J. Non-Newtonian Fluid Mech.* **2004**, *118*, 65−81.
(61) Venerus, D. C.; Kahvand, H. *J. Rheol.* **1994**, *38*, 1297−1315.
(62) Venerus, D. C.; Kahvand, H. *J. Polym. Sci., Part B: Polym. Phys.* **1994**, *32*, 1531−1542.
(63) Oberhauser, J. P.; Pham, K.; Leal, L. G. *J. Rheol.* **2004**, *48*, 1229−1249.
(64) Casson, N. In *Rheol. Disperse Systems*; Univ. Coll. Swansea, 1959; pp 84−104.
(65) Li, J.; Zhou, C.; Wang, G.; Yu, W.; Tao, Y.; Liu, Q. *Polym. Compos.* **2003**, *24*, 323−331.
(66) Lee, J. A.; Kontopoulou, M.; Parent, J. S. *Polymer* **2004**, *45*, 6595−6600.
(67) Xie, W.; Gao, Z.; Pan, W.-P.; Hunter, D.; Singh, A.; Vaia, R. *Chem. Mater.* **2001**, *13*, 2979−2990.
(68) Gelfer, M.; Burger, C.; Fadeev, A.; Sics, I.; Chu, B.; Hsiao, B. S.; Heintz, A.; Kojo, K.; Hsu, S. L.; Si, M.; Rafailovich, A. *Langmuir* **2004**, *20*, 3746−3758.
(69) Treece, M. A.; Oberhauser, J. P. *Polymer*, in press (DOI 10.1016/j.polymer.2006.12.029).
(70) Tanaka, H.; Meunier, J.; Bonn, D. *Phys. Rev. E* **2004**, *69*, 031404.
(71) Ren, S. Z.; Sorensen, C. M. *Phys. Rev. Lett.* **1993**, *70*, 1727−1730.
(72) Sollich, P. *Phys. Rev. E* **1998**, *58*, 738−759.
(73) Donth, E. *The Glass Transition: Relaxation Dynamics in Liquids and Disordered Materials*; Springer-Verlag: Berlin, 2001.
(74) de Gennes, P. G. *Scaling Concepts in Polymer Physics*; Cornell University Press: Ithaca, NY, 1979.
(75) Bonn, D.; Kellay, H.; Tanaka, H.; Wegdam, G.; Meunier, J. *Langmuir* **1999**, *15*, 7534−7536.

MA0612374